University of Zurich[UZH]

Zurich Open Repository and Archive
University of Zurich
University Library
Strickhofstrasse 39
CH-8057 Zurich
www.zora.uzh.ch

Year: 2008

How morphology affects self-assembly in a stochastic modular robot

Miyashita, S ; Kessler, M ; Lungarella, M

DOI: https://doi.org/10.1109/ROBOT.2008.4543751

Posted at the Zurich Open Repository and Archive, University of Zurich
ZORA URL: https://doi.org/10.5167/uzh-9418
Conference or Workshop Item

Originally published at:
Miyashita, S; Kessler, M; Lungarella, M (2008). How morphology affects self-assembly in a stochastic modular robot. In: IEEE International Conference on Robotics and Automation (ICRA 2008), Pasadena, CA, USA, 19 May 2008 - 23 May 2008. IEEE Computer Society, 3533-3538.
DOI: https://doi.org/10.1109/ROBOT.2008.4543751

2008 IEEE International Conference on
Robotics and Automation
Pasadena, CA, USA, May 19-23, 2008

How Morphology Affects Self-Assembly in a Stochastic Modular Robot

Shuhei Miyashita, Marco Kessler and Max Lungarella

Abstract— **Self-assembly is a process through which an organized structure can spontaneously form from simple parts. Taking inspiration from biological examples of self-assembly, we designed and built a water-based modular robotic system consisting of autonomous plastic tiles capable of aggregation on the surface of water. In this paper, we investigate the effect of the morphology (here: shape) of the tiles on the yield of the self-assembly process, that is, on the final amount of the desired aggregate. We describe experiments done with the real system as well as with a computer simulation thereof. We also present results of a mathematical analysis of the modular system based on chemical rate equations which point to a power-law relationship between yield rate and shape. Using the real system, we further demonstrate how through a single parameter (here: the externally applied electric potential) it is possible to control the self-assembly of propeller-like aggregates. Our results seem to provide a starting point (a) for quantifying the effect of morphology on the yield rates of self-assembly processes and (b) for assessing the level of modular autonomy and computational resources required for emergent functionality to arise.**

I. INTRODUCTION

Robots are an indispensable part of current manufacturing technologies. For macroscopic objects conventional automated pick-and-place operations are not only economical but are also reliable, fast, and accurate. Well-known examples are the construction of cell phones, electronic circuits, and cars. As the assembled objects grow in complexity and the employed components become smaller and more delicate, conventional robots hit a barrier because of their inherent difficulty in precisely manipulating small-sized parts entailing lower yields and higher fabrication costs. The possibility of using self-assembly for the fabrication of structures from given components (potentially with nano- or micrometer dimensions) has been suggested as a promising and viable solution to this problem [1]. Self-assembly is ubiquitous and many fascinating instances exist documenting its power, e.g., the formation of molecular crystals, the folding of nucleic acid, swarm behavior in ants or fish, and the formation of galaxies. It is plausible to assume that self-assembly can also lead to innovation in applications such as macro-scale multi-robot coordination and manufacturing technology for micro-scale devices.

In the field of modular robotics many attempts have been made to realize self-assembling and self-reconfigurable systems. Work has been mainly focused on the design and construction of basic building blocks of a typically small repertoire, with docking interfaces that allow transfer of mechanical forces and moments, and electrical power, and that can also be used for communication [2]–[13]. These robots can rearrange the connectivity of their structural units to create new topologies to accomplish diverse tasks. One way to classify current research on modular systems is according to the amount of planning and determinism required for generating a structure of interest. If the units move or are directly manipulated into their target locations through deliberate active motion, the modular system is "deterministically self-reconfigurable" implying that the exact location of the unit is known all the time, or can be calculated at run time.

If the units move around by other means (e.g., by exploiting surface tension or by taking advantage of Brownian motion), the system is "stochastically self-reconfigurable" implying variable reconfiguration times and uncertainties in the knowledge of the units' location (the location is known exactly only when the unit docks to the main structure). The advantages of this form of reconfiguration are at least two-fold: it can be extended to small scales and it alleviates local power requirements. To date a few self-reconfigurable modular robots relying on stochastic self-assembly have been built [14]–[19]. Although in all these systems the units interact asynchronously and concurrently, a certain amount of state-based control is still required for the modules to move, communicate, and dock. To our knowledge there have not yet been any attempts at exploring stochastic modular systems where parts have only limited (or no) computational (i.e. deliberative) abilities.

Such systems, however, are widespread in the biological world. The formation of the complex symmetrical protein shells of spherical viruses is a particularly familiar instance of self-assembly. The shell of the T4 phage, for instance, is composed of hundreds of parts and it is not plausible to assume that the instructions for its construction are contained in the virus' genetic material. It turns out that the shell consists of monomers that self-assemble without the need for a blueprint. Even more surprising, if one mixes the right kind of proteins the virus can be synthesized *in vitro* [20]. There are three basic issues with this picture: (1) although little is known about the underlying assembly process, the fact that all viruses adopt similar mechanisms hints at common design principles suggesting that simplified models (such as the one presented in this paper) might be helpful in understanding the process; (2) even for a small virus, there are too many possible intermediates to allow a complete description of the assembly process with three independent stages [20]; and (3) a generalized scheme has to exist to avoid a substantial

This research was supported by the Swiss National Science Foundation project #200021-105634/1 and EU FET-PACE project FP6-002035.

S. Miyashita, M. Kessler and M. Lungarella are with the Artificial Intelligence Lab, Dept. of Informatics, University of Zurich, Switzerland miya@ifi.uzh.ch

degree of incorrect assembly (yield problem).

In this paper we study more carefully the role played by the morphology (e.g., shape and material properties) of the individual modules with respect to the yield problem. More specifically, we use a stochastic modular robot called Tribolon as a tool to investigate this issue. One of the important aspects of our work is to develop a better formal understanding of the general principles underlying self-assembly as well as the role played by morphology. In the following section, we first describe our experimental system. Then, in Section III we report the results of experiments done with the real system, using a physics-based computer simulation, and obtained via mathematical analysis. We conclude the paper in Section IV by first discussing our results and by pointing to some future work.

II. Experimental Setup: Tribolon

To test our ideas, we used macroscopic modular units capable of moving on the surface of water. Each module consisted of a pie-shaped wedge spanning an angle of $\alpha = 60$ degrees made of durable plastic (acrylnitrile butadene styrene), a small pager motor (vibrator) positioned on top of the wedge, as well as a permanent magnet attached to the module's bottom surface and oriented orthogonally to the module's main axis (Fig. 1a). The magnet was made of Neodymium and had a surface magnetic flux density of $1.3\,T$. A pantographic system was used to supply the pager motor with energy (Fig. 1b). When an electrical potential was applied to the ceiling plate (made of aluminum), current flew through the pantograph to the pager motor returning to ground via electrodes immersed in the water ($83.3\,g/l$ of salt an (electrolyte) were added to the water to make it conductive). Because we used magnets (and not a mechanical docking system), we were able to build small and lightweight modules weighing approximately $2.8\,gr$ covering an area of $12.25\,cm^2$. A vibrating module is shown in Fig. 1c. Note that, as depicted in Fig. 1b, the modules can tilt inducing rather large fluctuations in the current flowing through the motors.

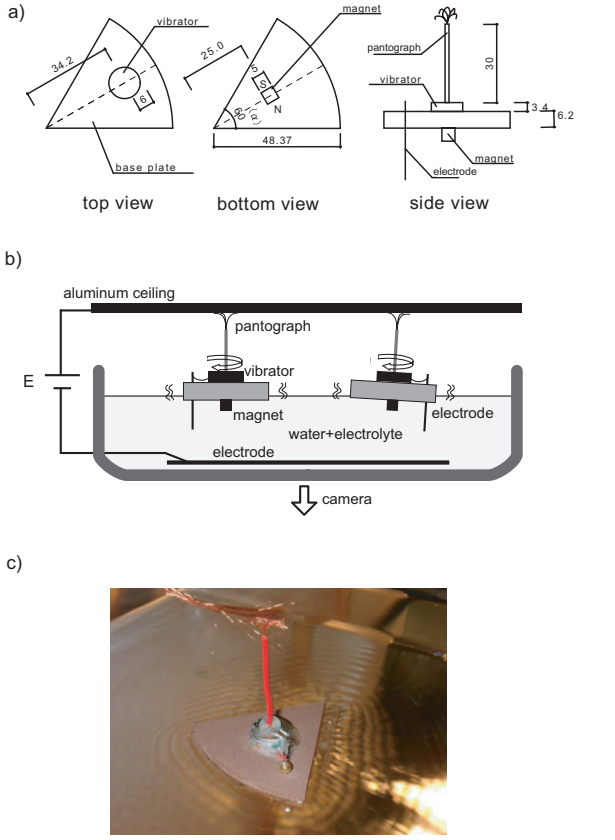

Fig. 1. Experimental setup. a) Schematic representation of a Tribolon module (units: $[mm], [degrees]$). Each module weighs approximately $2.8\,gr$ and covers an area of $12.25\,cm^2$. The angle spanned by the circular sector is $\alpha = 60$ degrees. b) Illustration of the experimental environment with two modules. c) Real module.

III. Results

A. Real System

Snapshots taken from three experiments using 6 modules are visualized in Fig. 2. In each experiment, a different (constant) electric potential was applied between the ceiling plate and the bottom submersed electrode causing the Tribolon modules to aggregate in various ways. In the experiment reproduced in Fig. 2 (bottom), we applied a potential of $E = 7\,V$. The modules first moved along random paths vaguely reminiscent of Brownian motion. After some time ($\approx 9\,sec$), through magnetic attraction, some of the modules were pulled to each other forming two-units clusters (X_2; here X_i stands for the state of a cluster consisting of i modules). These clusters further combined to generate a four-units cluster (X_4), then a five-units cluster (X_5), and eventually a six-units cluster (X_6) (sequential self-assembly; Fig.2). Once this final state was reached, the whole circular structure started rotating counter-clockwise at an approximately constant speed (like a rotor or a propeller). A plausible explanation for this "higher level functionality" can be found in the intermittency of the contact of the pantograph with the aluminum ceiling (due to the stable configuration of the 6-units cluster on the water surface; see Fig. 1b) which in turn leads to a pulsed current flow.

In the snapshots reproduced in Fig. 2 (center), the potential was set to $E = 8V$. As a result of the higher potential, the motors vibrated at a higher frequency increasing the likelihood of segregation of clusters while decreasing the likelihood of aggregation. Most of the time, all types of clusters disintegrated shortly after formation, exception made for the six-units cluster (X_6) which, due to its symmetry, proved to be a stable structure. It is important to note that the formation of the six-units cluster at $T = 98\,sec$ was accidental (one-shot self-assembly; Fig.2). This tendency, suppressing intermediate states, is thought to be a potential solution to the yield problem.

The snapshots in Fig. 2 (top) were obtained by applying a potential of $E = 9V$. This potential induced the pager motors to vibrate even faster making the formation of a six-units cluster unlikely. In fact, even for prolonged experiments

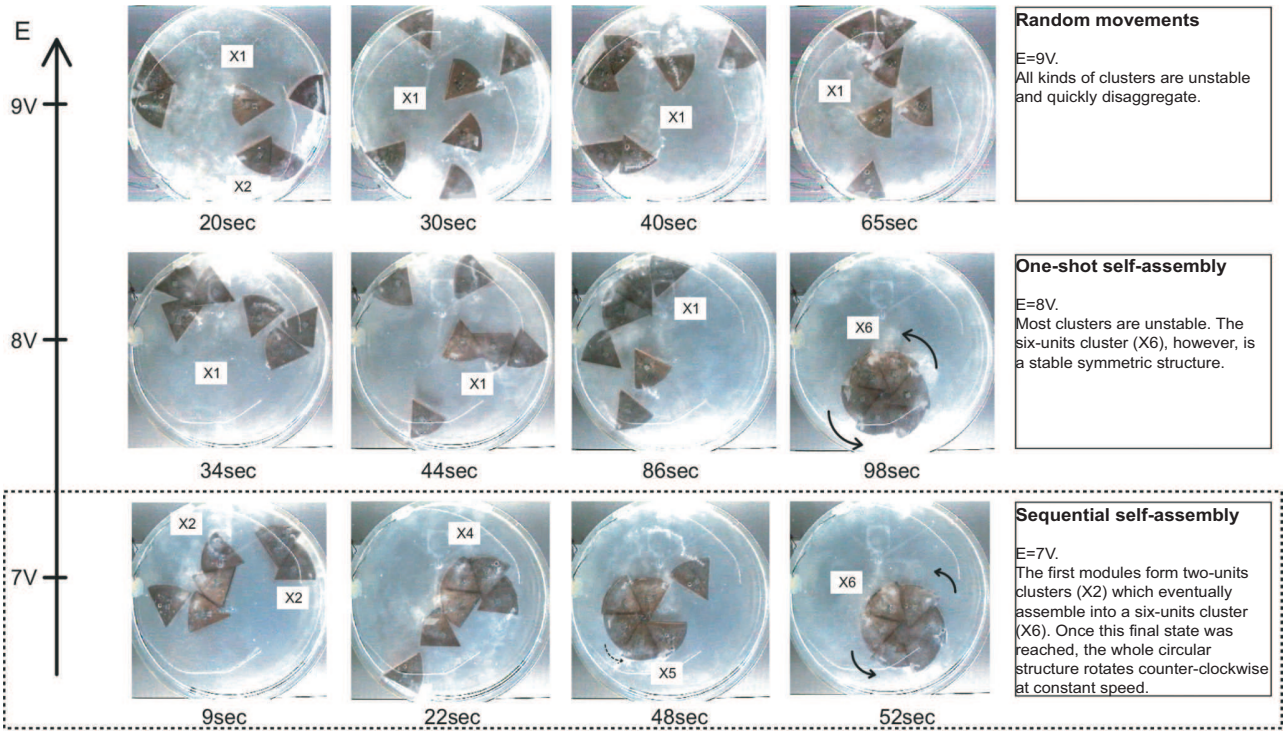

Fig. 2. Experimental results. Self-assembly process as a function of the applied electric potential E.

no clusters could be observed (random movements; Fig.2). We confirmed this result by initializing the experiment with modules arranged in a circular configuration consisting of six units (the desired configuration); as expected, the cluster was unstable and disaggregated shortly after the start of the experiment.

The problem of producing a desired configuration in large quantities (while avoiding incorrect assemblies) is known as the "yield problem" and has been studied in the context of biological and nonbiological self-assembly systems [21], [22]. For example, let us assume that the self-assembly process is initialized with 12 modules – each one a pie-shaped wedge spanning 60 degrees – with the objective to form two complete circles consisting each of 6 modules. In fact, the likelihood that the system actually settles into the desired configuration (a circle) is rather low (Fig. 3). An

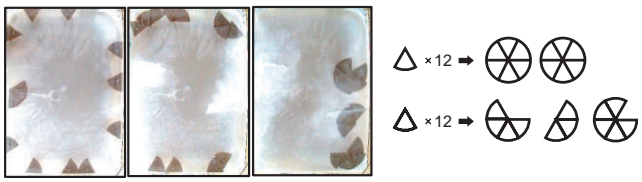

Fig. 3. Yield problem and stable clusters. Twelve circular sectors X_1 can aggregate into two X_6 clusters. In most cases, however, the modules organize themselves in more than three clusters. The yield in the upper part of the figure is 100%, the one in the lower part is 0%.

essentially analogous problem is investigated in the context of DNA folding where one of the objectives is to increase the yield rates of the self-assembly process [23]. Similarly, a lot of research effort is being devoted to the development of high yield procedures for integration and mass manufacturing of heterogeneous systems via self-assembly of mesoscopic and macroscopic components [24]–[26].

In order to investigate the interactions among many modules and to see how changes in the morphology (here: the angle) of the modules affect the convergence to the desired state and the yield rate, we conducted a computer simulation as well as mathematical analysis of the system. In particular, we focused on the case $E = 7V$ for which in the real system, few clusters disintegrated after having formed a six-units aggregate (see dotted box in Fig. 2).

B. Simulated System

The computer simulations were realized using the Ageia physics engine and the OGRE open source graphics engine [1]. The kinematic and dynamic parameters of the simulations were tuned manually so that the behavior of the simulated system matched relatively closely the one observed in the real system. The obvious advantages of a simulation are the possibility to explore the interaction between a large number of modules and the ease with which the morphology of the modules can be altered.

Snapshots of some of the simulations comprising 100 modules are reproduced in Fig. 4. As can be seen from the figures, the modules rather quickly aggregate into small-sized clusters (X_2 and X_3), and then later merge into bigger and more stable clusters (X_6). Modules in medium-sized clusters

[1] http://www.ageia.com/, http://www.ogre3d.org/

(X_4 and X_5) are exposed to less balanced force distributions, and consequently the formed clusters are most unstable (see also Fig. 7 d,e). Clusters composed of six units (X_6) are quite stable and the process reaches a yield rate of about 40% (that is, in average 40% of all modules belong to a six-units cluster). As described in the following section, this result can be confirmed by mathematical analysis.

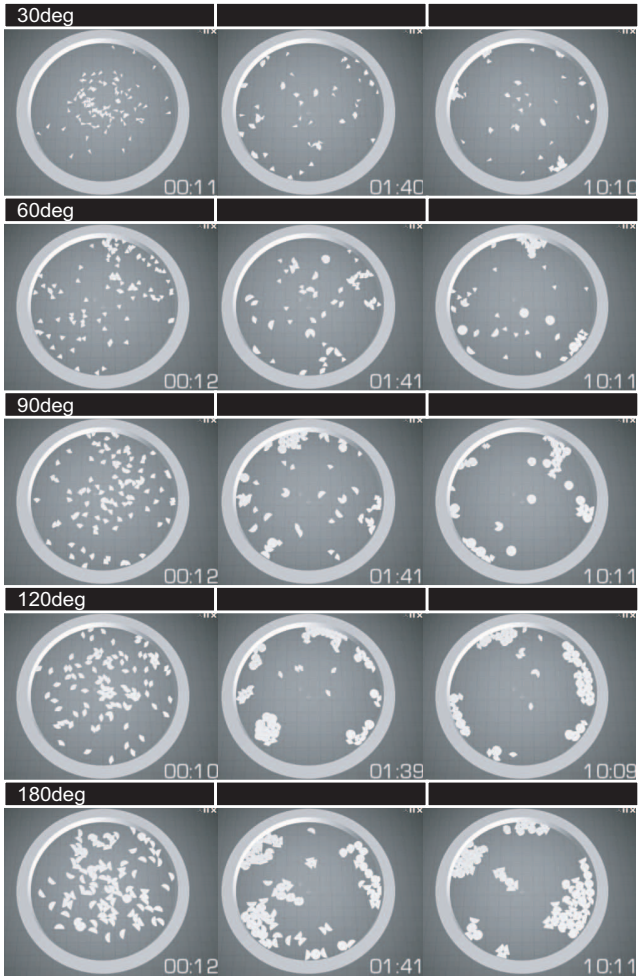

Fig. 4. Snapshots of computer simulation for modules spanning 30, 60, 90, 120, and 180 degrees.

C. Mathematical Model

We studied the behavior of our self-assembly system using kinetic rate equations derived from analogy with chemical kinetics [21]. For the analysis, the quantity of every intermediate product is represented with a state variable. One can then express the state transitions of the variables as:

$$\begin{array}{ll} 2\mathrm{X}_1 \rightarrow \mathrm{X}_2, & \mathrm{X}_1 + \mathrm{X}_2 \rightarrow \mathrm{X}_3, \\ \mathrm{X}_1 + \mathrm{X}_3 \rightarrow \mathrm{X}_4, & \mathrm{X}_1 + \mathrm{X}_4 \rightarrow \mathrm{X}_5, \\ \mathrm{X}_1 + \mathrm{X}_5 \rightarrow \mathrm{X}_6, & 2\mathrm{X}_2 \rightarrow \mathrm{X}_4, \\ \mathrm{X}_2 + \mathrm{X}_3 \rightarrow \mathrm{X}_5, & \mathrm{X}_2 + \mathrm{X}_4 \rightarrow \mathrm{X}_6, \\ 2\mathrm{X}_3 \rightarrow \mathrm{X}_6 & \end{array} \tag{1}$$

where X_i stands for the state of a cluster consisting of i modules (e.g., two single-unit modules X_1 can merge to form one cluster X_2). Our mathematical model assumes that not more than 2 units can aggregate into a cluster at the same time. The transition of the state vector $\boldsymbol{x} = (x_1, \ldots, x_6)$ obeys the following difference equation:

$$\boldsymbol{x}(t+1) = \boldsymbol{x}(t) + \boldsymbol{F}(\boldsymbol{x}(t)) \tag{2}$$

where x_i $(i = 1, \ldots, 6)$ is the number of clusters consisting of i units. Here t corresponds to time (more precisely: the number of collisions between clusters), and F is a transition function expressed as:

$$\begin{aligned} F_1(\boldsymbol{x}) &= (-2P_{11}x_1^2 - 2P_{12}x_1x_2 - 2P_{13}x_1x_3 - 2P_{14}x_1x_4 \\ &\quad - 2P_{15}x_1x_5)/S^2 \\ F_2(\boldsymbol{x}) &= (P_{11}x_1^2 - 2P_{12}x_1x_2 - 2P_{22}x_2^2 - 2P_{23}x_2x_3 \\ &\quad - 2P_{24}x_2x_4)/S^2 \\ F_3(\boldsymbol{x}) &= (2P_{12}x_1x_2 - 2P_{13}x_1x_3 - 2P_{23}x_2x_3 - 2P_{33}x_3^2)/S^2 \\ F_4(\boldsymbol{x}) &= (2P_{13}x_1x_3 + P_{22}x_2^2 - 2P_{14}x_1x_4 - 2P_{24}x_2x_4)/S^2 \\ F_5(\boldsymbol{x}) &= (2P_{14}x_1x_4 + 2P_{23}x_2x_3 - 2P_{15}x_1x_5)/S^2 \\ F_6(\boldsymbol{x}) &= (2P_{15}x_1x_5 + 2P_{24}x_2x_4 + P_{33}x_3^2)/S^2 \end{aligned} \tag{3}$$

where the probabilities P_{ij} represent the conditional probability of bonding on the condition that two units i and j collide. The coefficients are chosen by referring to Eq. 1 and by noting that the coefficient has a positive sign if X_i is a product, and has a negative sign if X_i is a reactant. The probabilities P_{ij} can be calculated using geometric considerations. Let us consider the case where two single units collide with probability P_{11}. We assume that these units will bond if (a) unit 2 is in the region S_1 of unit 1, and (b) unit 1 is in the region N_2 of unit 2 (Fig. 5); i.e., if the magnetic North pole of unit 2 (area N_2) faces the South pole of unit 1 (area S_1) or vice versa. The general equation is:

$$\begin{aligned} P_{ij} &= \frac{S_i}{S_i + N_i + B_i} \times \frac{S_j}{S_j + N_j + B_j} \times 2 \\ &= \begin{cases} \frac{1}{12\pi}(3\pi - 1.5S - 4a + 2\sin a) & S \leq 2(\pi - a) \\ \frac{1}{12\pi}(\frac{\sin\frac{\pi}{4}\cdot\sin a}{\sin(\frac{\pi}{4}-a)} - a) & S \geq 2(\pi - a) \end{cases} \end{aligned} \tag{4}$$

where S represents the sum of all the angles composing a cluster, and $a = \pi/4 - \arcsin(1/2\sqrt{2})$.

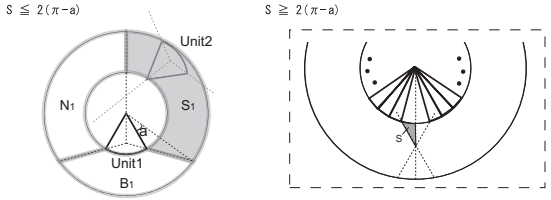

Fig. 5. Geometric relation of units.

Figure 6 displays the change over time of the number of clusters obtained by solving the system of difference

equations described above with initial condition $\boldsymbol{x}(0) = (100, 0, ..., 0)$. As can be seen in the figure, $X_5(t) > X_6(t)$, which exemplifies the "yield problem."

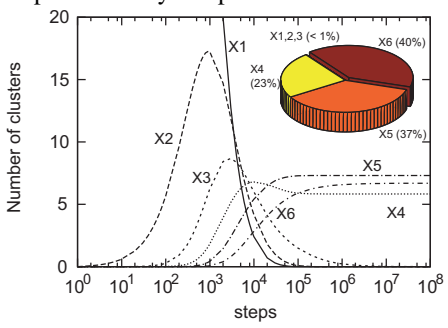

Fig. 6. Number of clusters as a function of time. The solution of Eq. 3 for the initial condition of $\boldsymbol{x}(0) = (100, 0, ..., 0)$. The yield problem is evident from the fact that at steady-state $X_5(t) > X_6(t)$. The yield rate of each cluster is listed on the top-right of the figure as a circle graph.

Figure 7 compares the results of the computer simulation with the ones obtained through mathematical analysis. Because the correspondence between "time" in the mathematical analysis and real time is not meaningful, we plotted the trajectories of the number of four, five and six-units clusters (X_4, X_5 and X_6) against the number of three-units clusters (X_3). The overall lower count of four-units clusters is a consequence of the instability of this particular structure. Any of the two units at the boundary of a four-units cluster (denoted by a white dot in Fig. 7e) can easily shift towards the center of the cluster. As soon as the distance between the two boundary units decreases, the identical polarities of the magnets will lead to a repulsive force and thus to a decomposition of the four-units cluster into one unit and a three-units cluster (Fig. 7d). In a five-units cluster, this sort of repulsive interaction is not as likely because boundary units can only rotate (and not shift) hence preserving the balance of forces (Fig. 7d).

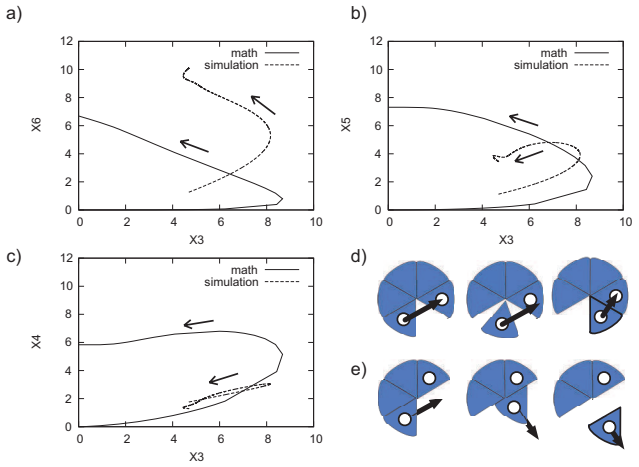

Fig. 7. Projections of the trajectory of the state variables (a-c) for mathematical analysis and simulation. Stability and instability of four-units and five-units clusters (d,e). "Boundary" units are indicated by white dots.

Figures 8 (a,b) show how shape changes affect the yield of the self-assembly process. The yield rates are normalized by multiplying them by the number of units required to construct a full circle (i.e., in the case of $\alpha = 60$ degrees the factor is 6; in the case of $\alpha = 180$ degrees units the factor is 2), and plotted as a function of the angle α. As can be seen in the figure, the yield rate falls off linearly with the angle. This result can be explained by considering that the number of clusters required to form the desired structure is inversely proportional to the angle. An additional point is that clusters formed by an even number of units show better yield rates. In Fig. 8 b, we plotted the yield rates on a logarithmic scale. As expected, the narrower the angle, the worse is the performance of the system. Interestingly, the relationship between yield rate and angle follows a power-law with a scaling exponent of 0.81. Although this will require additional support, we hypothesize that this relationship is a result of the shape of the module (in this case the circular sector with an orthogonally attached magnet).

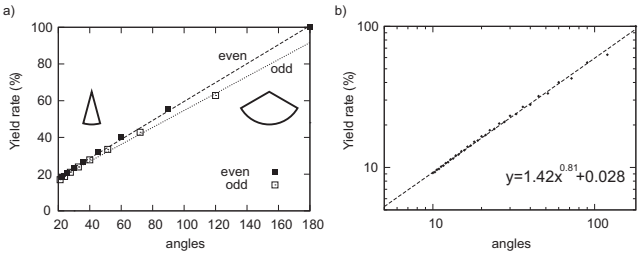

Fig. 8. Yield rates as a function of the angle spanned by the pie-shaped wedge; (a) linear scale and (b) logarithmic scale.

IV. Discussion

In this section we discuss some of the main points emerging from our experiments.

A. Levels of functionality

Let us return to the question formulated in the Introduction: can we build non-biological (modular) systems that self-assemble like biological ones? By carefully mapping the interaction networks of the approximately 70 proteins involved in the assembly of the T4 phage, one can observe that the aggregation processes are extremely well organized [20]. For instance, a protein A can only dock on a protein B by first coupling with a protein C: A+B+C $\rightarrow$ AC+B $\rightarrow$ ABC. It follows that through coupling with protein C, protein A can acquire a different level of functionality, which then enables the interaction with protein B. We assume that this kind of interaction networks can lead to emergence of multiple levels of functionality which play a crucial role in many morphogenetic processes. The formation of a propeller-like rotating aggregate (Fig. 2; $E = 7V$) is an instance of what one might call "emergent functionality."

B. Inertial vs viscous world

For objects in water at the mm scale, viscosity is as important as inertia (the Reynolds number, that is, the ratio of inertial forces and viscous forces, is ≈ 1). It follows that objects of $0.1\,mm$ dimensions scale are affected mostly by

viscous forces whereas objects of $1\,cm$ dimensions scale are affected mostly by inertial forces. For objects on the order of $1\,\mu\,m$ or less, such as bacteria, diffusion is a more effective way of locomotion than active propulsion (e.g., swimming bacteria are slower than diffusing molecules [27]). The implication for us is that we need to be careful when relating our work to small scales. Although at small scales, it might be possible to observe complete bottom-up self-assembly this might not be the case at large scales. Further work will be required to assess how our results can be mapped to smaller scales.

C. From low autonomy to mid-level autonomy

Focusing on the mechanisms of living things from a viewpoint of autonomous and distributed systems, it can be noticed that the components which form the morphology are not always highly autonomous [28]. Indeed, we could probably obtain the same results by employing modules without pager motors, but by supplying power through an external, rotating magnetic field. The key when we discuss autonomy of components in the context of autonomous-distributed systems might not be whether the units are passive or active, but whether the units are passive or "reactive." By drawing from our current experience in designing, constructing and controlling macroscopic modular systems, we hope that we will be able to derive conclusions about what the level of autonomy is needed to achieve self-assembly. One could say that life is a blind engineer, because the components – e.g., molecules – self-construct into organisms in a completely bottom-up fashion.

V. Conclusion

We proposed a novel type of stochastic modular system which can be induced to self-assemble through a single control parameter (externally applied electric potential). Using a real system, computer simulation, and mathematical modeling, we studied the effect of the morphology of the modules on the yield rate of the self-assembly process. Our results seem to indicate that computational resources can be traded off by appropriate morphology. We believe that the technological and conceptual advancements achieved recent with small-scale modular robots offer new and exciting opportunities to deepen both the realization and the theoretical understanding of scalable self-assembly systems. We hope that some of the principles discovered (e.g., concerning the dependence of self-organization on morphology of units) will also lead to a better understanding of similar processes found in natural systems.

VI. Acknowledgments

We would like to thank Rolf Pfeifer for the many helpful suggestions.

References

[1] Whitesides, G.M., Grzybowski, B.: Self-assembly at all scales. Science **295** (2002) 2418–2421

[2] Fukuda, T., Kawauch, Y.: Cellular robotic system (cebot) as one of the realizations of self-organizing intelligent universal manipulator. In: Proc. Int. Conf. on Robotics and Automation. (1990) 662–667

[3] Chirikjian, G.S.: Kinematics of a metamorphic robotic system. In: Proc. Int. Conf. on Robotics and Automation. (1994) 449–455

[4] Murata, S., Kurokawa, H., Kokaji, S.: Self-assembling machine. In: Proc. Int. Conf. on Robotics and Automation. (1994) 441–448

[5] Murata, S., Kurokawa, H., Yoshida, E., Tomita, K., Kokaji, S.: A 3-D self-reconfigurable structure. In: Proc. Int. Conf. on Robotics and Automation. (1998) 432–439

[6] Murata, S., Tomita, K., Yoshida, E., Kurokawa, H., Kokaji, S.: Self-reconfigurable robot. In: Proc. Int. Conf. on Intelligent Autonomous Systems. (1999) 911–917

[7] Yim, M.: New locomotion gaits. In: Proc. Int. Conf. on Robotics and Automation. Volume 3. (1994) 2508–2514

[8] Kotay, K., Rus, D., Vona, M., McGray, C.: The self-reconfiguring robotic molecule. In: Proc. Int. Conf. on Intelligent Robots and Systems. Volume 1. (1998) 424–431

[9] Rus, D., Vona, M.: Crystalline robots: Self-reconfiguration with compressible unit modules. Autonomous Robots **10**(1) (2001) 107–124

[10] Castano, A., Behar, A., Will, P.M.: The conro modules for reconfigurable robots. IEEE/ASME Trans. on Mechatronics **7**(4) (2002) 403–409

[11] Jorgensen, M.W., Ostergaard, E.H., Lund, H.H.: Modular atron: Modules for a self-reconfigurable robot. In: Proc. of Int. Conf. on Intelligent Robots and Systems. Volume 2. (2004) 2068–2073

[12] Zykov, V., Mutilinaios, E., Adams, B., Lipson, H.: Self-reproducing machines. Nature **435**(7039) (2005) 163–164

[13] Detweiler, C., Vona, M., Kotay, K., Rus, D.: Hierarchical control for self-assembling mobile trusses with passive and active links. In: Proc. Int. Conf. on Robotics and Automation. (2006) 1483–1490

[14] White, P., Kopanski, K., Lipson, H.: Stochastic self-reconfigurable cellular robotics. In: Proc. Int. Conf. on Robotics and Automation. Volume 3. (2004) 2888–2893

[15] White, P., Zykov, V., Bongard, J., Lipson, H.: Three dimensional stochastic reconfiguration of modular robots. In: Proc. of Robotics Science and Systems. (2005) 161–168

[16] Griffith, S., Goldwater, D., Jacobson, J.: Robotics: Self-replication from random parts. Nature **437** (2005) 636

[17] Shimizu, M., Ishiguro, A.: A modular robot that exploits a spontaneous connectivity control mechanism. In: Proc. Int. Conf. on Robotics and Automation. (2005) 2658–2663

[18] Bishop, J., Burden, S., Klavins, E., Kreisberg, R., Malone, W., Napp, N., Nguyen, T.: Programmable parts: A demonstration of the grammatical approach to self-organization. In: Proc. Int. Conf. on Intelligent Robots and Systems. (2005) 3684–3691

[19] Napp, N., Burden, S., Klavins, E.: The statistical dynamics of programmed self-assembly. In: Proc. Int. Conf. on Robotics and Automation. (2006) 1469–1476

[20] Leiman, P.G., Kanamaru, S., Mesyanzhinov, V.V., Arisaka, F., Rossmann, M.G.: Structure and morphogenesis of bacteriophage t4. Cellular and Molecular Life Sciences **60** (2003) 2356–2370

[21] Hosokawa, K., Shimoyama, I., Miura, H.: Dynamics of self-assembling systems: Analogy with chemical kinetics. Artificial Life **1**(4) (1994) 413–427

[22] Hosokawa, K., Shimoyama, I., Miura, H.: 2-d micro-self-assembly using the surface tension of water. Sensors and Actuators A **57** (1996) 117–125

[23] Rothemund, P.W.K.: Folding dna to create nanoscale shapes and patterns. Nature **440**(7082) (2006) 297–302

[24] Wolfe, D.B., Snead, A., Mao, C., Bowden, N.B., Whitesides, G.M.: Mesoscale self-assembly: Capillary interactions when positive and negitive menisci have similar amplitudes. Langmuir **19** (2003) 2206–2214

[25] Gracias, D.H., Tien, J., Breen, T.L., Hsu, C., Whitesides, G.M.: Forming electrical networks in three dimensions by self-assembly. Science **289** (2000) 1170–1172

[26] Boncheva, M., Ferrigno, R., Bruzewicz, D.A., Whitesides, G.M.: Plasticity in self-assembly: Templating generates functionally different circuits from a single precursor. Angew. Chem. Int. Ed. **42** (2003) 3368–3371

[27] Motokawa, T.: Time of an elephant, time of a mouse. CHUO-KORON-SHINSHA, INC. (1992)

[28] Alberts, B., Hohnson, A., Lewis, J., Raff, M., Roberts, K., Walter, P.: Molecular biology of the cell. Garland Science (2002)